# Northumbria Research Link

Northumbria
University
NEWCASTLE

# Preparation and characterization of layer-diffusion processed $InBi_2Se_4$ thin films for photovoltaics application

Nisar Ali [1,2*], R. Ahmed[2,**], Arshad Hussain[2,3], Yong Qing Fu[4,*], Murad Ali[1], Bakhtiar Ul Haq[5], S. AlFaify[5]

[1]Department of Physics, GPG Jahanzeb College Saidu Sharif Swat 19130, KPK, Pakistan
[2]Department of Physics, Faculty of Science, University Teknologi Malaysia, Johor, Malaysia
[3]Shenzhen Key Laboratory of Advanced Thin Films and Applications, College of Physics and Energy, Shenzhen University China
[4]Faculty of Engineering & Environment, University of Northumbria, Newcastle upon Tyne, NE1 8ST, UK

[5]Advanced Functional Materials & Optoelectronics Laboratory, Department of Physics, King Khalid University, Saudi Arabia.

Corresponding author. nisaraliswati@hotmail.com

**ABSTRACT**

In this research work, optoelectronic properties of Indium bismuth selenide ($InBi_2Se_4$) thin films are studied for their potentials for photovoltaic applications. The $InBi_2Se_4$ films are prepared via a thermal co-evaporation technique on glass substrate using $Bi_2S_3$ powders and indium granules. The as-deposited films are then annealed at different temperatures to convert into $InBi_2Se_4$ thin films. Results show that the obtained $InBi_2Se_4$ films possess excellent optoelectronic properties as an optimum bandgap of 1.2 eV was obtained for the film annealed at 350ºC. Based on characterisation results of current and voltage realiationships, both as-deposited and annealed $InBi_2Se_4$ thin films show a linear relationship between current and annealing temperature. It was also noted that with increasing grain-size of the film, the current is also increased at a fixed applied voltage.

.

**Keywords**: $InBi_2Se_4$; Thin films; Photovoltaics; Annealing; Diffusion;

## Introduction

$Bi_2Se_3$ has the potential of commercial production in a large area with low fabrication costs [1]. It is a topological insulator with a high surface conductivity and serves as an insulator in its bulk form. $Bi_2Se_3$ is commonly used in hole-transporting, and its crystallized phases can be easily processed using a solution method at room temperature [2, 3]. $Bi_2Se_3$ has been used extensively in photoelectrochemical (PEC) cells, solar selective decorative coatings, Hall magnetometers, photodiode arrays, and electrodes in solar cells [4, 5]. However, the high vapor pressure of selenium during the formation of the $Bi_2Se_3$ compound makes it very sensitive to substrate temperature. The Se vacancies in $Bi_2Se_3$ causes it having an n-type conductivity, and a dual conductivity is expected for $Bi_2Se_3$ with the controlled Se vapor pressure [6, 7].

Indium selenide is a binary compound with ~2 eV bandgap and an n-type conductivity. It is widely used in photovoltaic device fabrication as a window/absorbing layer, and exists in different phases such as InSe, $In_2Se_3$, $In_4Se_3$, $In_6Se_3$ [8]. It is also a layered semiconductor and can be easily deposited using electrodeposition technique, molecular beam epitaxy, flash evaporation, and chemical vapor deposition [9]. A moderate annealing temperature around 100°C is capable of achieving crystallization of InSe thin film deposited by co-thermal evaporation techniques. The conductivity of InSe is controllable with the thickness of the material though a grain boundary scattering mechanism. However, it is noted that the indium rich film has large defects densities, as a result, the carrier recombination process is increased and thus the device efficiency is reduced [10, 11]. It has many potential technological applications such as "phase-change random access memory (PRAM)" devices, solar cells, photosensors, buffer layer material, wide energy range photo-detectors, and lithium-ion batteries [12, 13]. Moreover, InSe has dual conductivity and dual bandgap (direct and indirect) depending upon growth conditions and intercalation circumstances and doping [14].

Although $Bi_2Se_3$ and InSe have shown potential applications in technology especially in photovoltaics, both of them need further improvement for their high-quality applications in the state of the art commercial technologies. Due to the current interest in chalcogenide materials and their potential in optoelectronic and photovoltaic properties, we will focus on our work to achieve a high performance and single ternary compound of $InBi_2Se_4$ thin films [15]. In this paper, we report the properties of chalcogenide-based $InBi_2Se_4$ materials for solar cell

applications by depositing the above two layers via thermal evaporation techniques, the obtained $InBi_2Se_4$ thin films are characterized to be a good absorbing layer material for thin-film solar cell technology.

## Experiment

Indium bismuth selenide (IBS) thin films were fabricated using co-evaporation techniques using a thermal coater (Edward 306) from $Bi_2Se_3$ 99.99% pure powder heated at 600°C and indium granules heated at 155°C. The distance between the source and substrate was adjusted to be ~8 cm while the pressure of the chamber was maintained at $\sim 2\times10^{-5}$ mbar. For the deposition process, soda-lime glass was used as a substrate which was washed carefully with deionized water plus acetone in an ultrasonic bath. The annealing of the obtained thin films was performed at 150°C, 250°C, and 350°C for 1 hour in a vacuum furnace. The structural analysis was done using an X-ray diffractometer (X-ray D-8 Discover XRD) with a CuKα radiation (with an X-ray wavelength of 1.54 A) as an energy source. A 4-probe Keithley Source Meter (Keithley 2400) was used for the current and voltage (I-V) characterization. Optical properties of the films were explored using a UV-VIS spectrometer. To obtain compositions and chemical bonding information of the films, an X-ray photoelectron spectrometer (XPS, Kratos Axis Ultra) was used, with Al $K_\alpha$ radiation (1486.6 eV) source.

## Results and Discussion

XRD pattern of the as-deposited and annealed indium bismuth selenide thin films are shown in Figure 1. The as-deposited films are nearly amorphous because only few crystalline peaks are present in the pattern. The only focal peak in the as-deposited film is at (-312) while the other peaks are at (711) are minor ones. However, with the increasing annealing temperatures, the films show their polycrystalline nature. The film annealed at 150°C show the best quality of XRD peaks. At an annealing temperature of 250°C, a few strong diffraction peaks start appearing which indicates that the crystallization with annealing is enhanced, e.g., (-514) and (-111) peaks. For the sample annealed at 350°C, more strong diffraction peaks for $InBi_2Se_4$ were observed as can be seen from Figure 1.

The crystalline size *D* of the thin film annealed at 350°C (peak position θ=27.099°) and peak broadening ($\beta$) can be calculated by the method of Williamson-Hall analysis [16, 17].

$$\beta = \frac{K\lambda}{D\cos(\theta)} + \varepsilon \tan(\theta)$$

where *K* is used for Scherrer's constant (0.9), $\lambda$ is a symbol used for the wavelength (Cu monochromatic Kα lines, λ= 1.54060 Å) and $\varepsilon$ represents the microstrain of the crystal while *D* stands for the crystallite size. When $\beta\cos(\theta)$ is plotted as a function of 4 sin ($\theta$), a straight line is attained (figure 2). The slope of this line is used to determine the micro-strain of the crystallites, while the average crystallite size is determined from the intercept [17]. The relation, $\delta = \frac{1}{D^2}$ is used to determine the line defects corresponding to the density of the dislocation. The surface density of the crystallite (N) can be measured by using the equation of $N = \frac{t}{D^3}$, where *t* represents the film thickness. The average thickness of the film was measured around 750 nm using a quartz crystal monitor during the deposition. The above mentioned results for the material structural parameters are tabulated in Table 1.

**Table 1:** Structural parameters of the annealed sample of the $InBi_2Se_4$ thin film at 350°C.

| No | Parameters | Value |
|---|---|---|
| 1 | Crystallite size (*D*) | 116.18 Å |
| 2 | Strain ($\epsilon$) | $9.2\times10^{-3}$ |
| 3 | Dislocation density (δ) | $7.43\times10^{15}$ nm$^{-2}$ |
| 4 | Number of crystallite per unit area (*N*) | $11.996\times10^{5}$ nm$^{-2}$ |

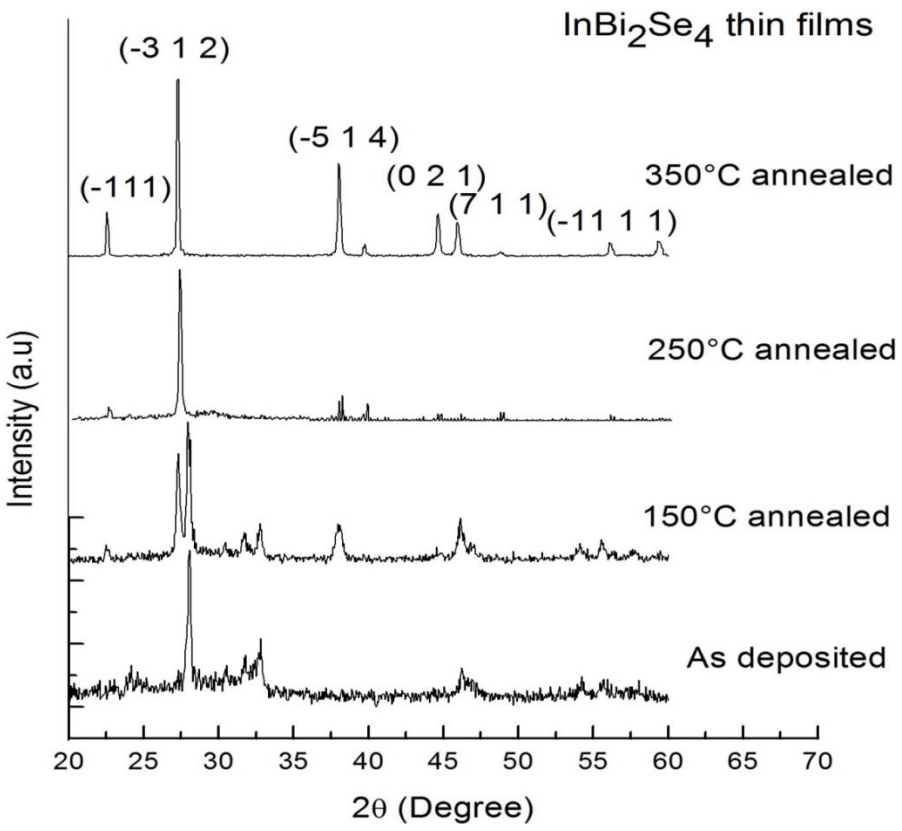


**Figure 1:** XRD analysis for Indium bismuth selenide

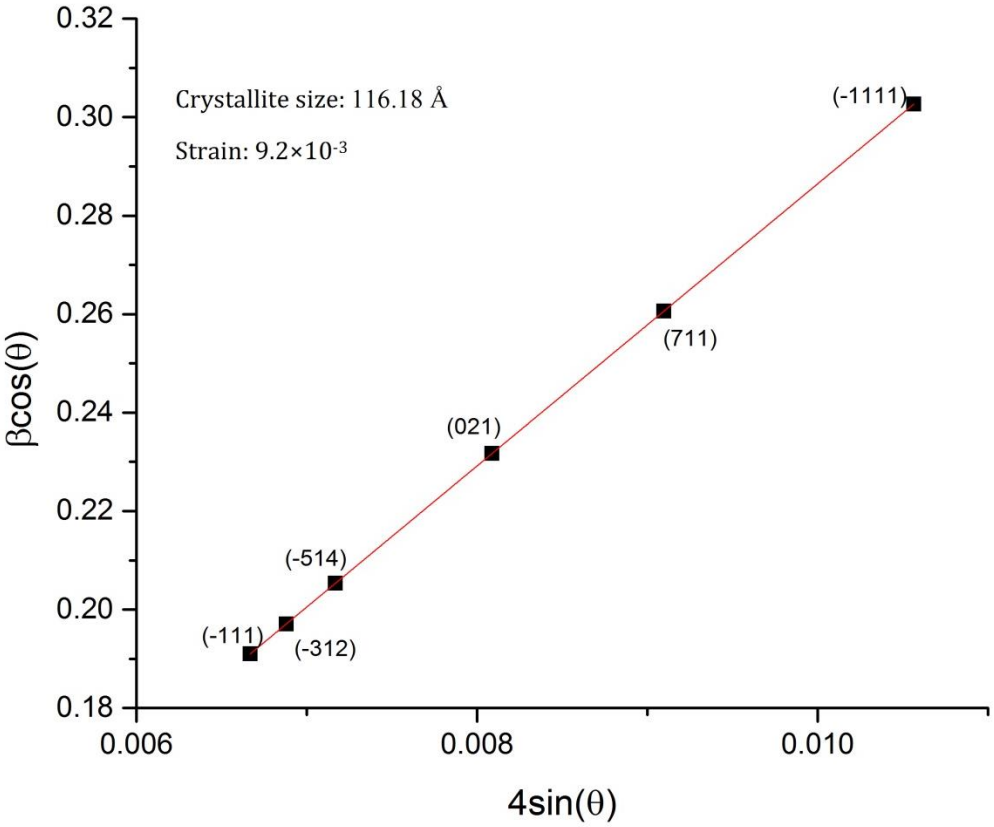


**Figure 2:** Williamson-Hall analysis of IBS films. The crystallites size is approximately 11.6 nm.

**Table 2:** Crystallographic data for $InBi_2Se_4$

| | |
|---|---|
| Space group | Monoclinic |
| a (Å) | 20.83200 |
| b (Å) | 4.1140 |
| c (Å) | 11.95800 |
| Volume | 903.61 $Å^3$ |
| Crystal size | 116.18 Å |

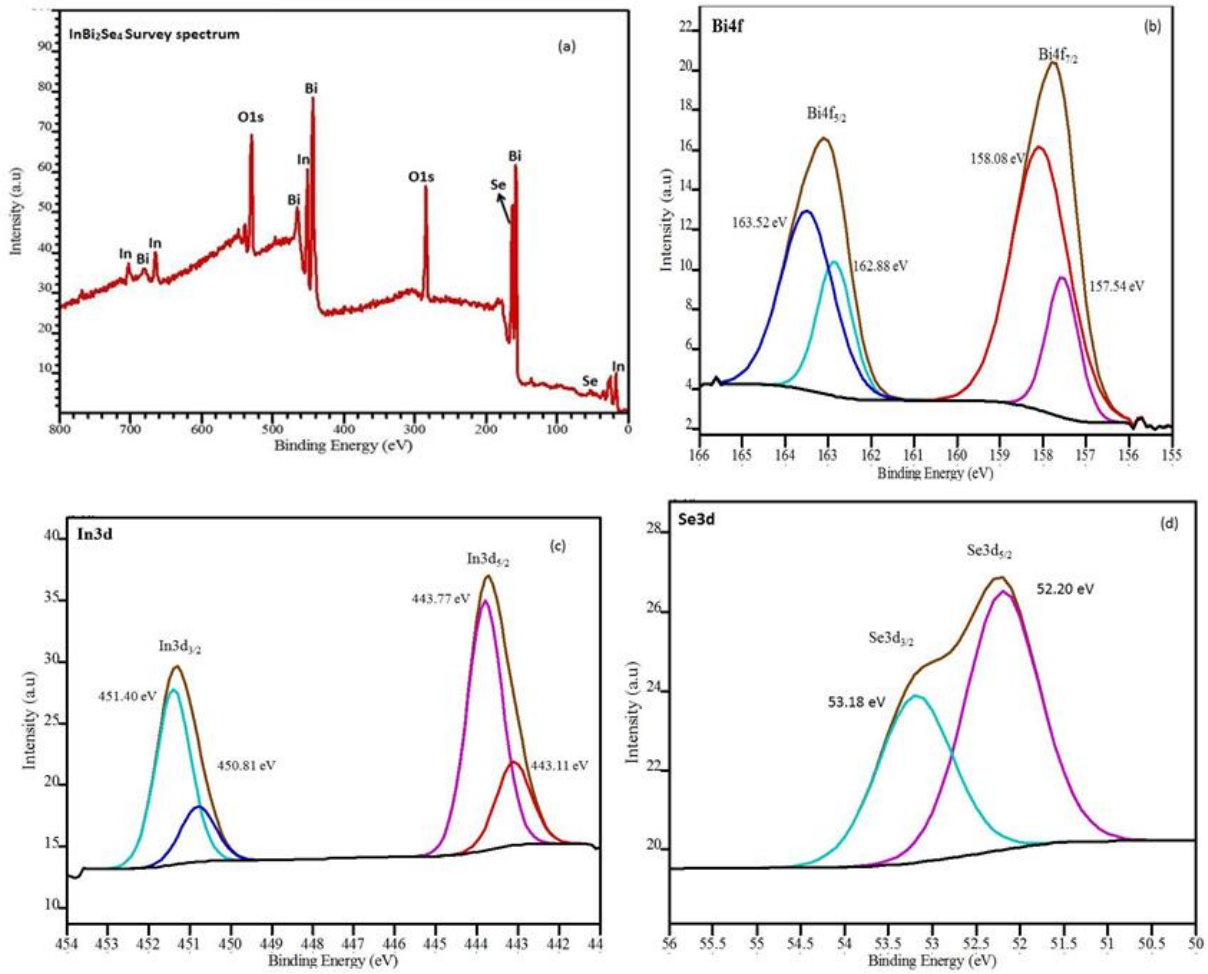


**Figure 3 (a-d):** The high-resolution XPS spectra of the identified three main elements; (a) survey spectrum; (b) Bi 4f; (c) In 3d; and (d) Se 3d

XPS analysis was performed for the determination of chemical bonding of the synthesized $InBi_2Se_4$ films. Figure 3(a) shows a typical survey spectrum of the $InBi_2Se_4$ annealed thin films at 350°C in which Bi, In and Se elements are found.. The bismuth high resolution spectrum at the core level of a 4f doublet state is shown in Figure 3(b)**.** The peaks corresponding to the 4f doublet state were found at 163.1 and 157.76 eV which are consistent with the reported XPS data of $Bi_2Se_3$. The above mentioned binding energies with a peak separation energy value of 5.34 eV correspond to doublet state Bi-$4f_{7/2}$ and Bi-$4f_{5/2}$. The peaks are found at 163.52 eV and 162.88 eV for Bi $4f_{5/2}$, and those for Bi $4f_{7/2}$ are at 158.08 eV and 157.54 eV, respectively. Due to surface adsorption, the component peaks associated with Bi-O, with a peak separation of

5.42 eV, are found to be positioned at 163.52 eV and 158.08 eV, respectively [18, 19]. Oxidation is found as a common problem in these Bi thin chalcogenide films [1]. Figure 3(c) shows a high-resolution XPS spectrum of the In, and the major peaks are observed at 443.7 eV and 451.3 eV with a difference of energy 7.6 eV between the peaks. These peaks are in the binding energy range of In $3d_{3/2}$ and In $3d_{5/2}$ for $In3^{+}$, respectively, suggesting $In^{3+}$ nature of the synthesized $InBi_2Se_4$ annealed thin films after annealed at 350°C. The peaks found at the positions of 52.2 eV and 53.18 eV correspond to Se 3d3/2 and Se 3d5/2, respectively, with a peak separation of 0.98 eV. These XPS data are comparable with the available data reported in the literature [20]. The binding energy values corresponding to the Se 3d are within the energy range (52-53 eV), which was estimated for the selenide phase in Figure 3(d). The proportion ratio of the peaks obtained for In (3p), Bi (4f), and Se (3d) is found 1:2:4, indicating the formation of $InBi_2Se_4$ thin films. These obtained XPS results are in a good agreement with XRD results of the thin film annealed at a temperature of 350 ˚C.

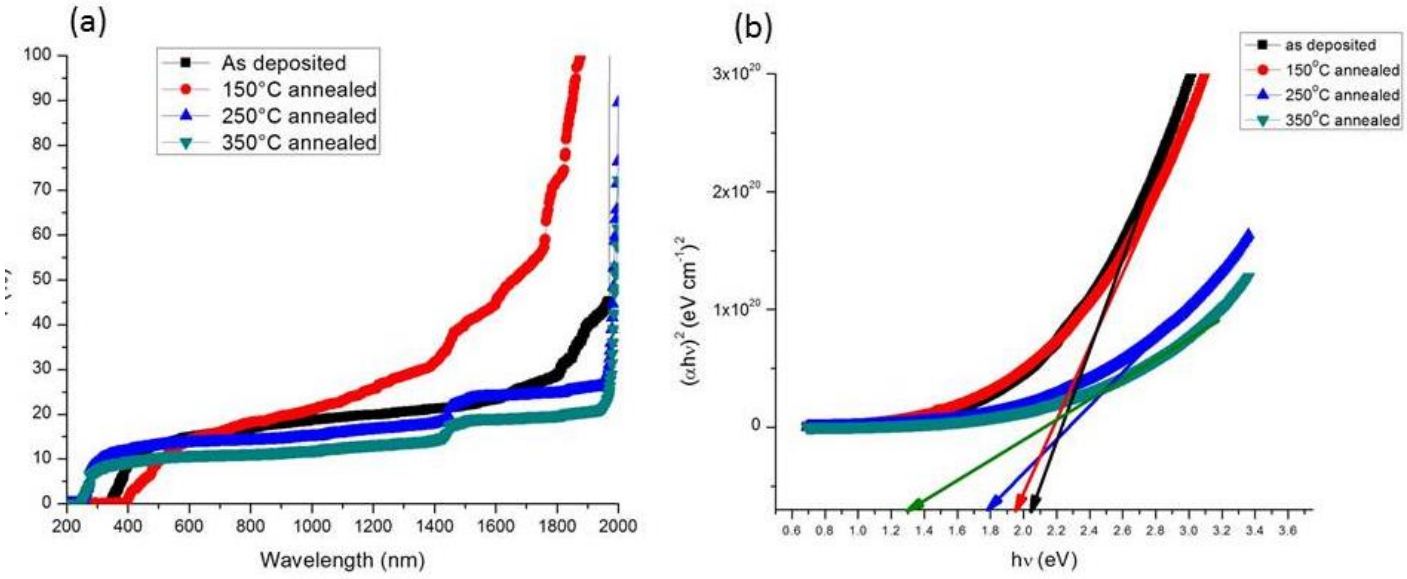


**Figure 4:** (a) Transmittance spectra $InBi_2Se_4$ (b) Band gap calculation.

Figure 4(a) shows the spectroscopic results obtained via UV-Vis spectroscopy which shows the transmittance spectra of the annealed and as-deposited thin films of $InBi_2Se_4$. InBi was reported as semi-metallic material in nature with an optical bandgap of 1.5 eV at 300°C [20]. However, the addition of selenium has transferred its semi-metallic nature to a semiconductor one with a

high degree absorption. The transmittance spectra shown in figure 4(a) for the annealed and as-deposited samples show clearly the good transmittance region above visible and IR wavelength range. It shows that the transmittance becomes decreased with increase of the annealing temperature. A maximum decrease, in the transmittance spectra, was noted at the 350°C annealed sample.

To calculate the bandgap [21], the absorption coefficient (α) of the annealed and as-deposited thin films is determined by using the following relation:

$$\alpha = \frac{1}{d} \ln \left(\frac{I_o}{I}\right) \quad (1)$$

$$\alpha h\nu = A(h\nu - E_g)^n \quad (2)$$

where d denotes thin film thickness, $I_o$ and I are used for the intensities of the incident and transmitted light while in equation (2), hν represents the photon energy, A and n are transition constant and transition coefficient (where n=1/2 and n=2 for the direct and indirect allowed bandgap transition). Figure 4(b) shows the obtained plot between $(\alpha h\nu)^2$ vs. hν which is used for estimating the bandgap energy. To do so, the linear part of the plot is extrapolated to zero-abscissa which intercepts the x-axis [12, 22]. The values of the bandgap energy for the samples annealed at 150°C, 250°C, and 350°C are 1.95 eV, 1.78 eV, and 1.3 eV, respectively, whereas the as-deposited thin film sample has a bandgap value of 2.05 eV. The decrease in the bandgap energy with annealing temperature is due to an increase in the grain size and the improved crystallinity of the annealed films.

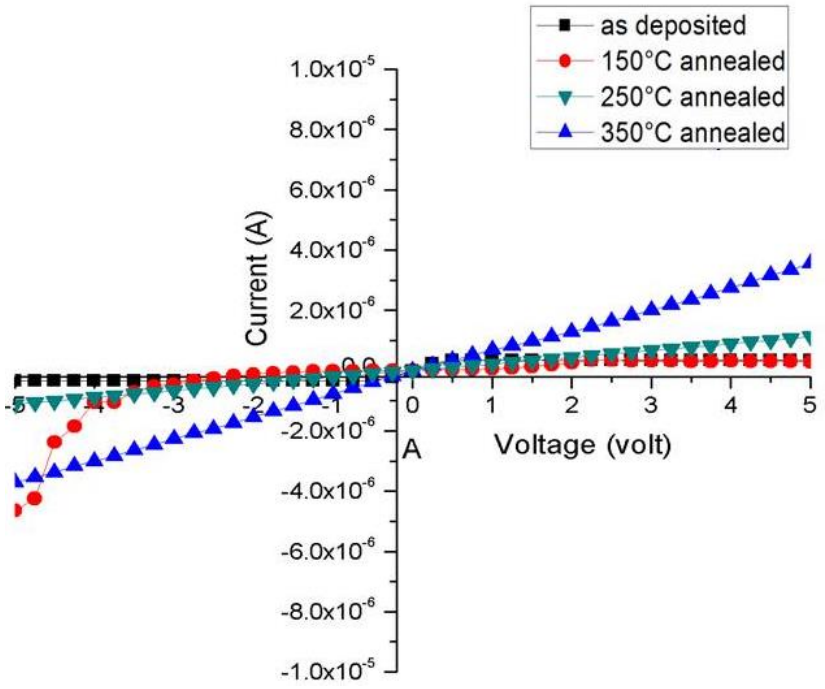


**Figure 5**: The current-voltage characteristics $InBi_2Se_4$ thin films.

The current-voltage graphs for the annealed and as-deposited samples of the thin films of $InBi_2Se_4$ are illustrated in Figure 5**.** The rectilinear correlations between current and annealing temperatures can be obtained for all the samples with an incremental rise of current with respect to the applied voltage. The increase in the current with respect to the applied voltage is an outcome of the increased crystallinity and crystallite size with the icnrease of annealing temperature. With the rising annealing temperature, the density of the grain boundaries is decreased and the carrier concentrations are increased, therefore, the electrical conductivity of the annealed thin films is also increased.

**Conclusions**

$InBi_2Se_4$ thin films were grown on glass substrates using thermal evaporation techniques. Structural and optoelectronic properties of the as-deposited thin films and those annealed at 150°C, 250°C and 350°C were studied. The films annealed at 350°C were found to have an orthorhombic polycrystalline crystal structure with highly oriented texture. The nature of the chemical bonding of the synthesized $InBi_2Se_4$ thin films along with their binding energies was

studied using the XPS. The deconvolution plots for the Bi revealed the high oxidation levels due to surface contamination and $In^{3+}$ nature of the synthesized $InBi_2Se_4$ films. The optical study was carried out in the spectral range 200–2000 nm for thin films. The energy gap was found to be decreased with increasing annealing temperature, indicating that the optical absorption in these films follow the rule of direct transitions. The bandgap of 1.3 eV obtained for the 350°C annealed thin film indicates its excellent photovoltaic property. The good electrical conductivity of the films i.e. a current of 4 μA at a voltage of 5V for the annealed thin film annealed at 350°C also shows that the obtained $InBi_2Se_4$ film is a good photovoltaic material.


1. Lai, Y.-H., et al., *Fabrication of a ZnO film with a mosaic structure for a high efficient dye-sensitized solar cell.* Journal of Materials Chemistry, 2010. **20**(42): p. 9379-9385.
2. Cui, H., et al., *Synthesis of Bi2Se3 thermoelectric nanosheets and nanotubes through the hydrothermal co-reduction method.* Journal of Solid State Chemistry, 2004. **177**(11): p. 4001-4006.
3. Sun, Y., et al., *Atomically Thick Bismuth Selenide Freestanding Single Layers Achieving Enhanced Thermoelectric Energy Harvesting.* Journal of the American Chemical Society, 2012. **134**(50): p. 20294-20297.
4. Waters, J., et al., *Deposition of bismuth chalcogenide thin films using novel single-source precursors by metal-organic chemical vapor deposition.* Chemistry of Materials, 2004. **16**(17): p. 3289-3298.
5. Ali, Z., et al., *Effect of synthesis technique on electrochemical performance of bismuth selenide.* Journal of Power Sources, 2013. **229**: p. 216-222.
6. Navrátil, J., et al., *Conduction band splitting and transport properties of Bi2Se3.* Journal of Solid State Chemistry, 2004. **177**(4–5): p. 1704-1712.
7. Hor, Y.S., et al., *$p$-type ${\text{Bi}}_{2}{\text{Se}}_{3}$ for topological insulator and low-temperature thermoelectric applications.* Physical Review B, 2009. **79**(19): p. 195208.
8. Madugu, M., et al., *Preparation of indium selenide thin film by electrochemical technique.* Journal of Materials Science: Materials in Electronics, 2014. **25**(9): p. 3977-3983.
9. Darwish, A.A.A., M.M. El-Nahass, and M.H. Bahlol, *Structural and electrical studies on nanostructured InSe thin films.* Applied Surface Science, 2013. **276**: p. 210-216.
10. El-Sayed, S.M., *Space-charge-limited current, trap distribution, and optical energy gap in amorphous (In13Se87 and In20Se80) thin films.* Vacuum, 2002. **65**(2): p. 177-184.
11. Viswanathan, C., et al., *CURRENT–VOLTAGE STUDIES ON VACUUM EVAPORATED In70Se30 THIN FILMS.* Journal of Optoelectronics and Advanced Materials, 2005. **7**(2): p. 713-720.
12. Su, Z., et al., *Fabrication of Cu2ZnSnS4 nanowires and nanotubes based on AAO templates.* CrystEngComm, 2012. **14**(3): p. 782-785.
13. Yan, Y., et al., *Influence of indium concentration on the structural and optoelectronic properties of indium selenide thin films.* Optical Materials, 2014. **38**: p. 217-222.
14. Pathan, H.M., et al., *Preparation and characterization of indium selenide thin films from a chemical route.* Materials Chemistry and Physics, 2005. **93**(1): p. 16-20.

15. Augustine, S. and E. Mathai, *Growth, morphology, and micro indentation analysis of Bi2Se3, Bi1.8In0.2Se3, and Bi2Se2.8Te0.2 single crystals.* Materials Research Bulletin, 2001. **36**(13–14): p. 2251-2261.
16. Law, M., et al., *ZnO−Al2O3 and ZnO−TiO2 Core−Shell Nanowire Dye-Sensitized Solar Cells.* The Journal of Physical Chemistry B, 2006. **110**(45): p. 22652-22663.
17. Velea, A., et al., *In-situ crystallization of GeTe\GaSb phase change memory stacked films.* Journal of Applied Physics, 2014. **116**(23): p. 234306.
18. Xu, F., et al., *Hierarchical ZnO Nanowire−Nanosheet Architectures for High Power Conversion Efficiency in Dye-Sensitized Solar Cells.* The Journal of Physical Chemistry C, 2010. **114**(6): p. 2776-2782.
19. Akhtar, M.S., et al., *Controlled synthesis of various ZnO nanostructured materials by capping agents-assisted hydrothermal method for dye-sensitized solar cells.* Electrochimica Acta, 2008. **53**(27): p. 7869-7874.
20. Abdin, Z., et al., *Solar energy harvesting with the application of nanotechnology.* Renewable and Sustainable Energy Reviews, 2013. **26**(0): p. 837-852.
21. Galca, A.C., et al., *Structural and optical properties of optimized amorphous GeTe films for memory applications.* Journal of Non-Crystalline Solids, 2018. **499**: p. 1-7.
22. Ali, N., et al., *Structural and optoelectronic properties of antimony tin sulphide thin films deposited by thermal evaporation techniques.* Optik - International Journal for Light and Electron Optics, 2013. **124**(21): p. 4746-4749.